Bulletin of Engineering Geology and the Environment (2019) 78:6143–6157
https://doi.org/10.1007/s10064-019-01523-0

ORIGINAL PAPER

Study on the failure mechanism and stability control measures in a large-cutting-height coal mining face with a deep-buried seam

De-Zhong Kong [1,2,3,4] · Zhan-Bo Cheng [5] · Shang-Shang Zheng [1]

Received: 21 October 2018 / Accepted: 4 April 2019 / Published online: 17 May 2019

Abstract

Coal face spalling is a major issue affecting the safety of a large-cutting-height mining face, especially in deep mining. In order to analyze failure mechanisms and propose corresponding stability control measures in a large-cutting-height longwall face, panel 1303, with a mining depth of 860 m, which is arranged and advanced distances of 300 m and over 1000 m along the dip and strike directions of a coal seam, respectively, was selected as the engineering background. In addition to uniaxial compressive strength (UCS) tests, triaxial compression tests under different confining pressures and loading methods were carried out to investigate the deformation characteristics of the coal specimens. A mechanical model, the "coal face support roof", was established to illustrate the factors affecting the stability of the coal face. Combined with numerical simulation, the dominant factor was obtained, and the stress distribution around the coal face at different advance distances was revealed. Based on the coal face failure mechanism, the pertinent in situ measures of "manila + grouting" reinforcement technology for controlling coal face spalling were proposed. The results showed that the coal face spalling depended mainly on vertical cyclic loading and horizontal unloading in both initial and periodic weighting. In terms of deep mining, the surrounding stress distribution played a vital role in coal face failure and instability. Specifically, two dimensions of loading conditions were found in the front 3 m of the coal face, and the principal stress σ_{xx} of the coal body was significantly less than the other two principal stresses in the front 8 m of the coal face. In addition, the horizontal principal stress σ_{yy} was greater than the vertical principal stress σ_{zz}. Therefore, the horizontal principal stress and strength of the coal body were the prominent influencing factors in the large-cutting-height coal face. The mining height and support system working resistance were also of great importance with respect to the stability of the coal face to some degree. Lastly, "manila + grouting" reinforcement technology proposed in this study resulted in 70–80% reduced potential for the occurrence of coal face spalling and in the degree of failure of the coal face, as well as grouting cost could be saved of 30–40% compared with pure grouting measures.

Keywords Deep-buried seam · Large cutting height · Failure mechanism · Stability control measures

Highlights
(1) Proposed coal face failure mechanism and transfer process of a stress state
(2) $\sigma_{yy} > \sigma_{zz} > \sigma_{xx}$ in the front 8 m of a coal face.
(3) Illustrated the main constraints and secondary factors affecting the stability of a coal face.
(4) Proposed a new technology, "manila + grouting" reinforcement into a coal face.

✉ Zhan-Bo Cheng
Z.Cheng.4@warwick.ac.uk

De-Zhong Kong
dzkong@gzu.edu.cn

Shang-Shang Zheng
gs.sszheng17@gzu.edu.cn

[1] College of Mining, Guizhou University, Guiyang 550025, Guizhou, China

[2] Guizhou Coal Mine Design and Research Institute, Guiyang 550025, Guizhou, China

[3] School of Resource and Safety Engineering, China University of Mining and Technology (Beijing), Beijing 100083, China

[4] Key Laboratory of Safety and High-efficiency Coal Mining, Ministry of Education (Anhui University of Science and Technology), Huainan 232001, Anhui, China

[5] School of Engineering, University of Warwick, Coventry CV47AL, UK

Introduction

With the acceleration of comprehensive mechanization of mining and rising coal demand, numerous coal mines have gradually been extended to deep-buried mining. For example, the depth of exploitation or expansion of various mining areas in China has now exceeded 800 m, and even 1000 m in Jiangsu and Shandong provinces (Wang et al. 2017). However, as a result of the high pressure, high temperature and high stress characteristics inherent in deep mining, it is more prone to the occurrence of various dynamic disasters (Aguado and González 2009; Zhao et al. 2017; Christopher 2016; Iannacchione and Tadolini 2016; Mazaira and Konicek 2015; Zhou et al. 2015; He et al. 2015). For example, it is easier for roof failure and collapse to occur due to high crustal stress in deep mines. The coal seam dip angle also influences the stability of the coal mining face and the law of surface subsidence (Yao et al. 2017; Alejano et al. 1999; Asadi et al. 2004). In addition, support systems cannot be fully mobilized, causing weak stability at the end of the working face, and exacerbating the degree of coal face spalling due to the larger cutting height (Huang et al. 2011). In recent years, sudden coal face spalling and roof collapse have been recognized as a prominent issue restricting the stope stability in deep-buried seams and larger-cutting-height mining faces (Kong et al. 2017; Suorineni et al. 2014; Peng and Chiang 1984). According to the comprehensive work regarding the failure type for coal face spalling by early on-site technicians, the key point in controlling coal face failure is focused on improving the corresponding support system measurements, such as acoustic emission (ACE) guard equipment. With the successful application of large-cutting-height mining technology, numerous scholars have undertaken extensive research on failure mechanisms and prevention technology for coal mining faces, and have tackled some problems of coal face spalling disasters (Chang et al. 2015; Li et al. 2015; Pang and Wang 2017; Wang et al. 2014; Wang et al. 2016; Gao and Stead 2014; Gao et al. 2014a, b; Lisjak and Grasselli 2014; Kazerani 2013; Zhang and Einstein 2004; Li et al. 2016; Fan et al. 2015; Xuan et al. 2016). A systematic study investigating the failure mechanism and control technology of coal face spalling revealed two main failure types: shear failure and tensile failure (Wang et al. 2015). It was determined that the intrinsic coal face failure was the destruction of the wedge sliding body. In addition, the failure area of the coal body was obtained using slip line theory to establish a mechanical model based on field measurements (Wang et al. 2017). For effective and efficient control of sudden coal face spalling and roof collapse, the "manila + grouting" method of reinforcement technology was proposed, and was been adopted and verified in an inclined, fully mechanized, top-coal caving mining face and a large-cutting-height mining face (Yang and Kong 2015; Yang et al. 2015).

Clearly, current research is more focused on the fields of theoretical analysis and practical application to control coal face failure. However, obtaining the general failure mechanism of a coal face is preferred, rather than considering the specific influencing factors such as mining depth or mining and boundary conditions. For deep mining in particular, horizontal stress cannot be neglected as a factor influencing the stability of a coal mining face. Therefore, combining theoretical analysis, numerical simulation and field measurement, this paper investigates the failure mechanism and stability control measures for a deep coal mining face, fully taking into account the horizontal stress and mining conditions.

Engineering background

The coal seam no. 13, with an almost horizontal buried depth of 860 m and average thickness of 5.0 m, is the main coal seam of panel 1303, which is arranged and advanced along the dip and strike directions of the coal seam a total of 300 m and over 1000 m, respectively. Backward longwall mining and roof caving methods have been adopted in the whole mining process as shown in Fig. 1. Additionally, Fig. 2 shows the geologic column of panel 1303, which indicates that the roof and floor strata are composed mainly of mudstone, carbonaceous mudstone, sandy mudstone and fine sandstone. However, the main floor also consists of local soft rock with a thickness of 2.5–5.5 m.

Failure mechanism of a deep-buried coal mining face

Coal face spalling and roof caving occur frequently in the mining of panel 1303 and have serious consequences, causing a slow advance of 1.5 m per day. Also, massive coal or rock

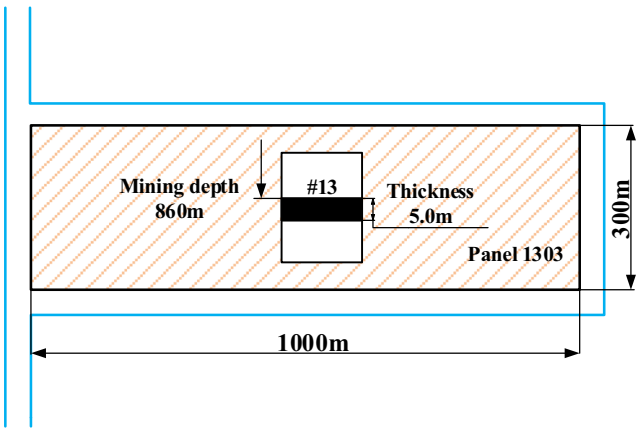

Fig. 1 Schematic layout of panel 1303

Column	Stratum	Lithology	Thickness/m
	Main roof	Fine sandstone	4
	Immediate roof	Mudstone and sandy mudstone	2
	Coal seam	Coal body	5
	Immediate floor	Sand and mud interbedding	3

Fig. 2 The integrated histogram of coal and rock

masses falling on transport equipment can significantly reduce the serviceability and service life of equipment, and threaten personal safety. Therefore, an understanding of the failure mechanism is critical in order to develop corresponding stability control measures in deep-buried large-section mining faces.

Failure characteristics of the coal face

Based on the observation and images of panel 1303 in different locations each day, the types of coal face failure are summarized and sorted out, as shown in Fig. 3. A part of the top zone and overall zone shear failure on the coal face are revealed to be a result of the relative weakness of coal and the rock mass. The direction of main stress changes, as the horizontal stress is generally greater than the vertical stress in a deep mine.

Failure mechanism of coal face spalling

Coal face spalling occurs in cycles as boundary conditions change continuously throughout the mining process. Coal face failure is related to the stress distribution influenced by the cyclical process of loading and unloading of confining pressure during each periodic weighting around the coal face. An MTS815 test system was used to investigate the deformation and failure of coal samples with triaxial and uniaxial tests considering confining pressure and loading modes. The partial coal specimens are shown in Fig. 4, and the stress–strain curves under different loading conditions are represented in Fig. 5.

Figure 5 demonstrates that peak strength reaches 50 MPa when the axial strain is 2.5%, followed by residual strength of 30 MPa until the axial strain reaches 6%, with a confining pressure of 12 MPa, in the triaxial loading test. In the triaxial unloading test, the peak and residual strength of the coal sample are reduced to 40 MPa and 20 MPa, with axial strain of 1.5% and 2%, respectively. In terms of cyclic loading, the peak and residual strength of the coal sample is about 20 MPa and 12.5 MPa, with axial strain of 2% and

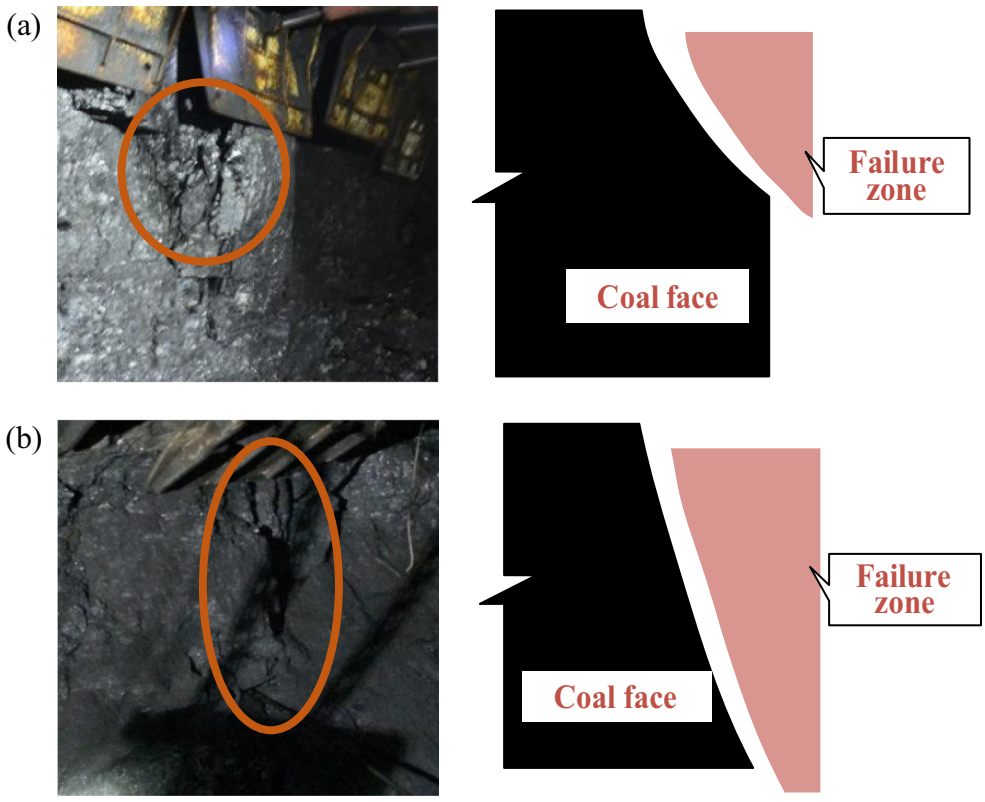

Fig. 3 Failure features of coal face spalling with top failure and overall failure

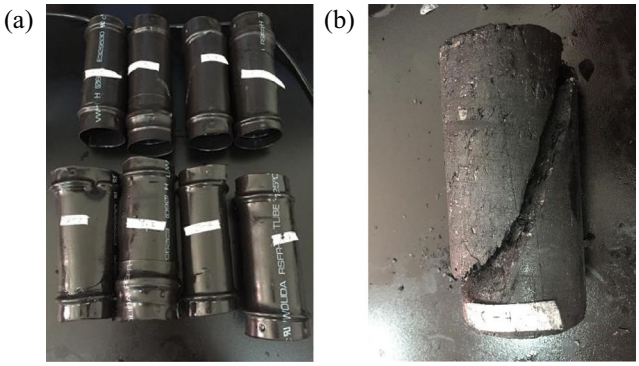

Fig. 4 Partial coal specimens: (a) intact specimens, (b) failure specimens

2.5%, respectively, when the confining pressure is also 12 MPa. However, there is a significant decrease in the peak and residual strength in uniaxial loading, with values of 8 MPa and 2.5 MPa, and axial strain of 0.5% and 1%, respectively.

Based on the data illustrated above, the coal mining face from the open cut to the initial weighting is in a three-dimensional stress state. This corresponds to the results of Fig. 5(a) which suggest that coal face spalling is unlikely to happen in this process. With the working face advancing continuously, it is determined that the confining pressure and ultimate strength of the coal body gradually decrease, corresponding with the results of Fig. 5(b). Meanwhile, the coal face is in dynamic development with cyclic loading and unloading in the axial direction, keeping the confining pressure constant in the support movement process, causing the strength of the coal face to weaken. For certain special geological conditions, the coal body is even in a one-dimensional stress state, corresponding to the results of Fig. 5(d), with the lowest failure strength for the coal mass. Therefore, the stress state around the coal face plays a vital role in the failure strength and features of the coal face. Throughout the process, from the open cut to the initial weighting or the duration of two periodic weightings, the stress state presents gradually increasing axial pressure and decreasing confining pressure, causing weakening of the coal body failure strength, leading to easy occurrence of coal face spalling.

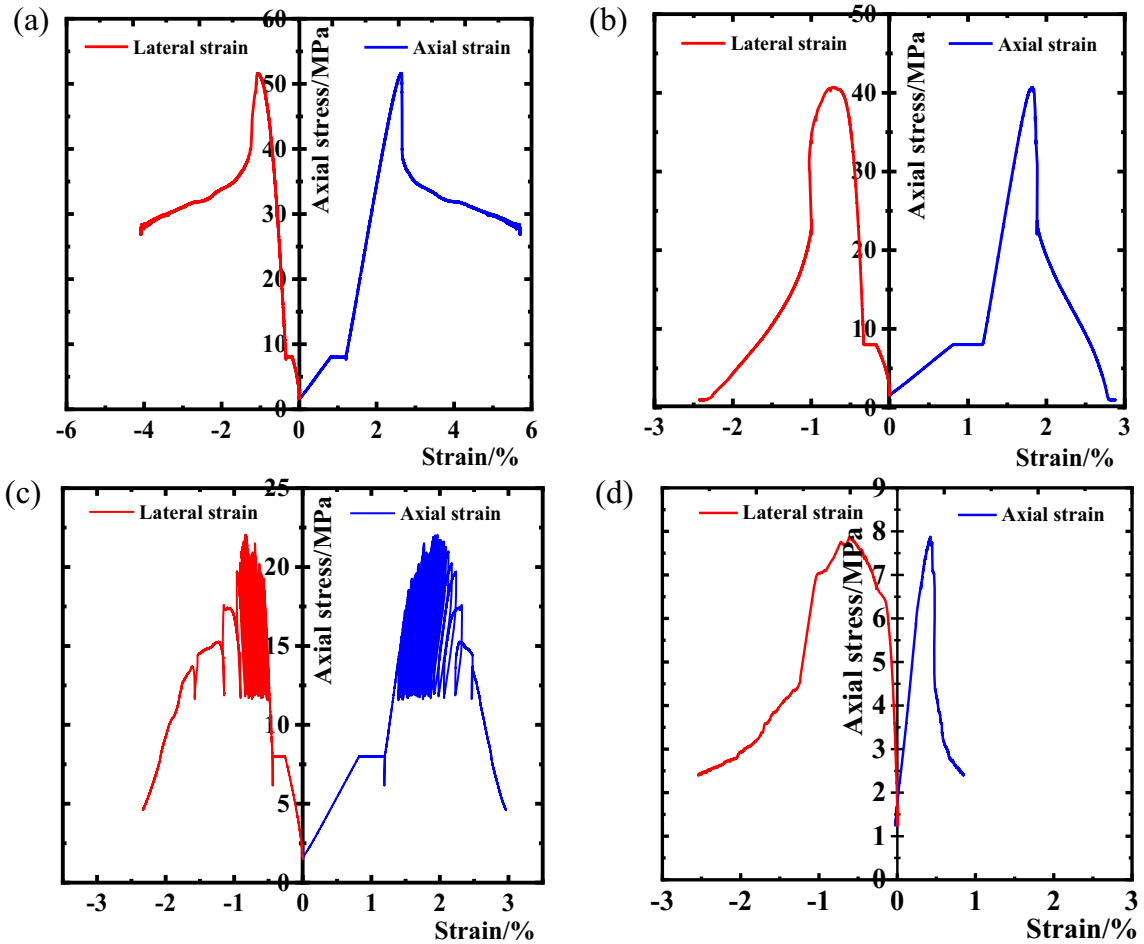

Fig. 5 Stress–strain curves of coal samples with different loading conditions: (a) triaxial loading, (b) triaxial unloading confining pressure, (c) cyclic loading, (d) uniaxial loading

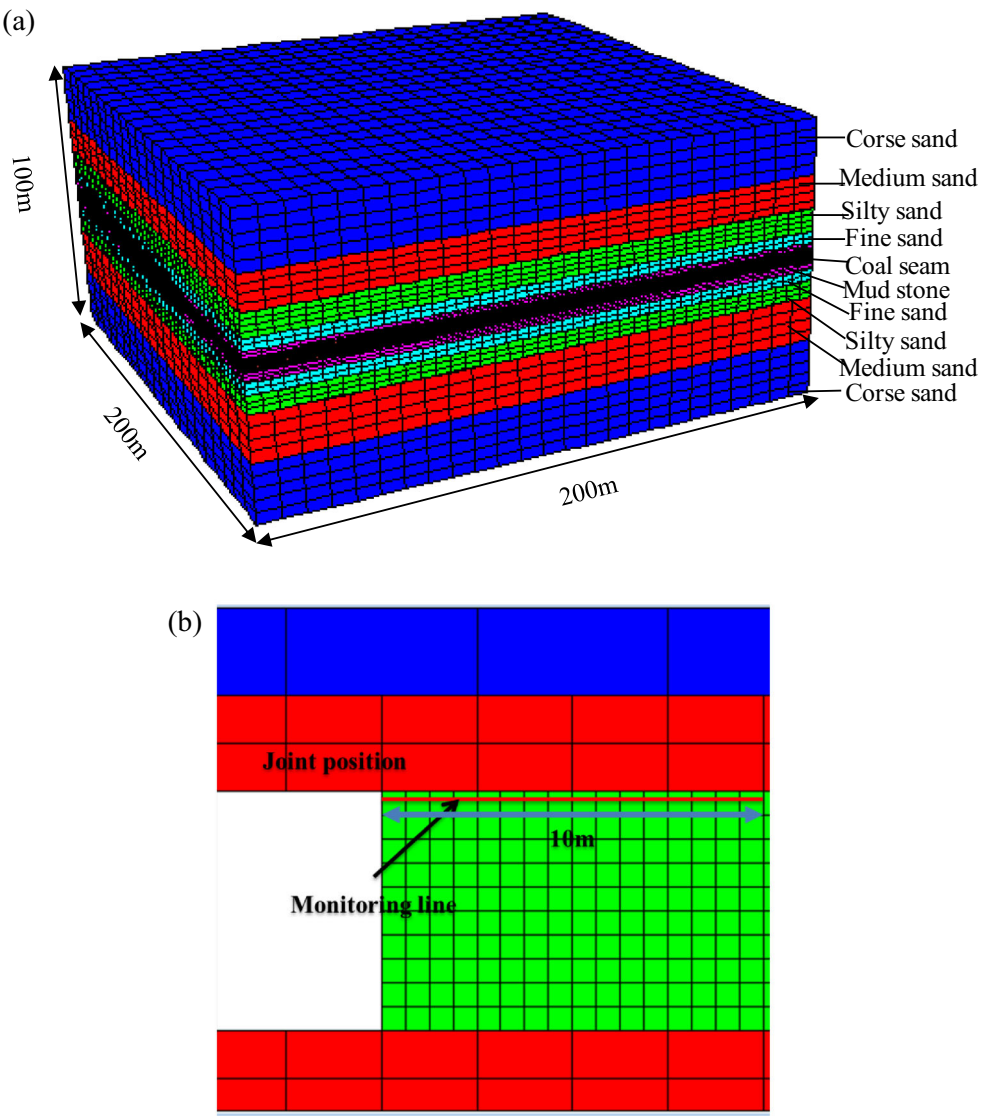

Fig. 6 Numerical model

Analysis of the coal face stress environment

Model establishment

In order to determine the failure mechanism of a large-cutting-height working face with a deep-buried coal seam, taking panel 1303 as an engineering background, numerical simulation was used to analyze the stress environment of the coal face under different advance distances by using FLAC3D [Fast Lagrangian Analysis of Continua in 3 Dimensions] software. Therefore, a model 200 m long, representing the advance distance, 200 m wide and 100 m in height was established with horizontal displacement restriction on the front, back, left and right planes, and vertical displacement restriction on the bottom plane as

Table 1 Mechanical parameters of coal and rock mass

Rock	Density (kg/m^3)	Cohesion (MPa)	Internal friction angle (°)	Volume modulus (GPa)	Shear modulus (GPa)	Tensile strength (MPa)
Coarse sandstone	2368	5.84	43	10.12	9.65	5.08
Medium sandstone	2500	5.9	42	7.38	6.96	4.56
Siltstone	2540	5.2	40	6.85	5.47	3.86
Fine sandstone	2600	4.38	39	5.27	4.69	3.35
Mudstone	2550	1.24	37	4.16	2.83	3.02
Seam	1350	0.5	30	3.95	2.2	1.04

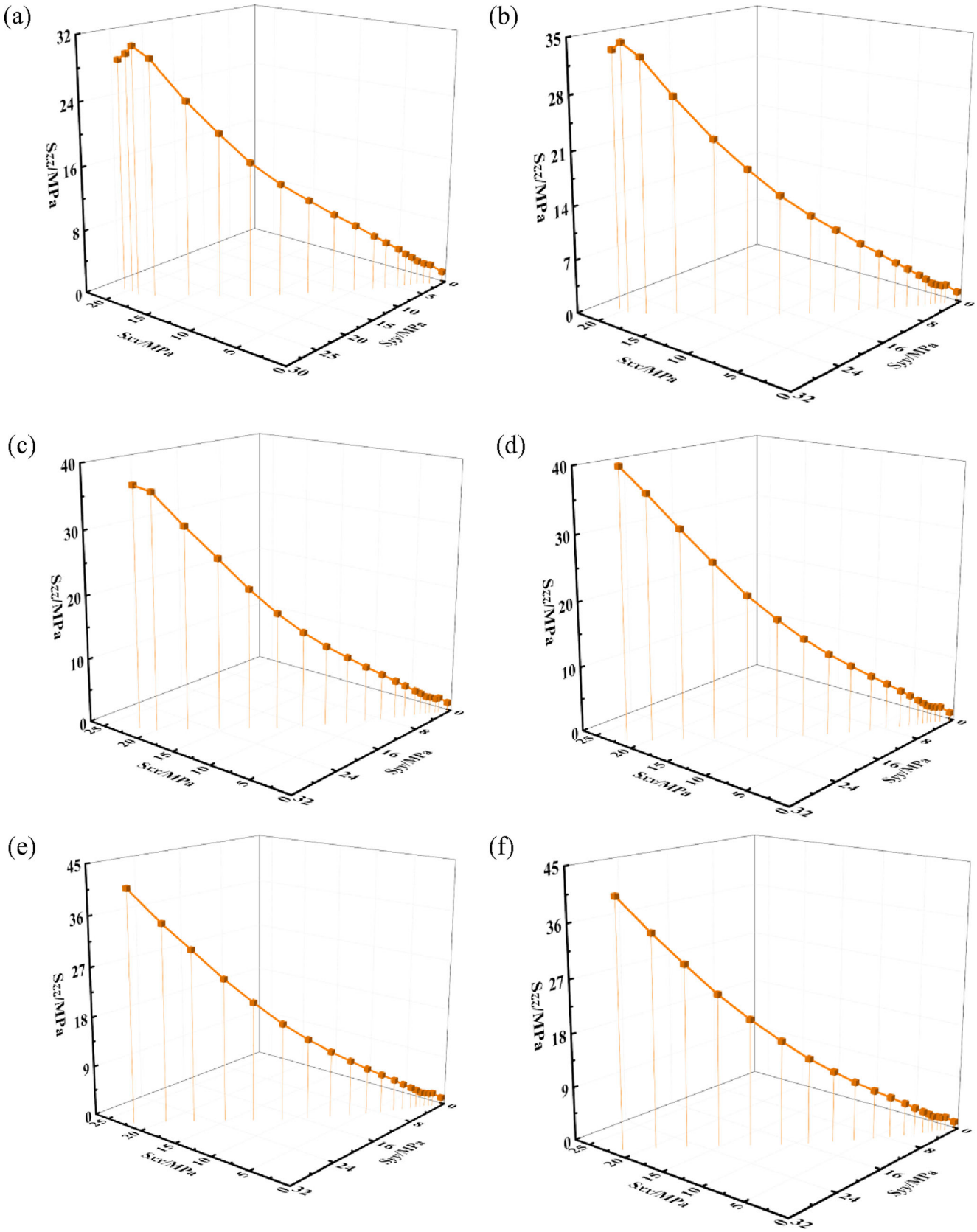

Fig. 7 Stress environment of coal face with different advance distances: (a) 10 m, (b) 20 m, (c) 30 m, (d) 40 m, (e) 50 m, (f) 65 m

shown in Fig. 6. Moreover, because the buried depth of the coal seam is 860 m, and the rock strata above panel 1303 in this model is just 60 m thick, a vertical stress of 20 MPa was applied on the top plane as gravity compensation to simulate the remaining height of stratum when a bulk density of 25 kN/m^3 was adopted for the overlying strata. At the same time, a monitoring line was set up with 10 m in the joint position between the coal mining face and immediate roof. Physical and mechanical parameters of the coal and rock mass were obtained through laboratory tests. The tests were conducted on the TAW-2000 controlled testing system with maximum axial load of 2000 kN, maximum shear load of 500 kN, and maximum lateral pressure of 500 kN. The uniaxial compressive strength, elastic modulus, and Poisson's ratio were obtained by conducting uniaxial compression tests, while the cohesion and friction angle were estimated by conducting triaxial compression tests. For each specific geological parameter, three specimens were tested to obtain an average value. The mechanical parameters based on the results of these tests are shown in Table 1.

Simulation results and discussion

Figures 7 and 8 illustrate the monitoring results of three-dimensional stresses in the front of the coal face at different advance distances and plastic failure zones, respectively.

The principal stress in the x direction within 2 m of the coal face is far less than the other two principal stresses due to excavation causing unloading in the x direction. In addition, the minimum value of σ_{xx} is less than 1 MPa. The principal stress σ_{yy} in the horizontal direction within 7.5 m from the working face is greater than the principal stress σ_{zz} in the vertical direction, while the opposite results are found beyond 7.5 m from the coal face.

Vertical stress can be regarded as the maximum principal stress, with a value of 30.78 MPa 9 m from the coal face when the advance distance is 10 m. However, the peak point of the maximum principal stress gradually moves away from the coal face with the working face continuously advancing, and its value also increases to 41.62 MPa with an advance distance of 50 m where the initial weighting occurs. The maximum principal stress is 41.17 MPa with an advance distance of 65 m, which indicates the occurrence of the first periodic weighting; as a result, the periodic weighting distance is 15 m.

Therefore, it is concluded that the coal body within a range of 3 m in the front of the coal face is basically loaded in two dimensions. The horizontal principal stress σ_{yy} is greater than the vertical principal stress σ_{zz}, followed by the principal stress σ_{xx} if the range extends to 8 m. In addition, the behavior of the floor is intense in a large-cutting-height mining face with a deep-buried seam; as a result, a serious degree of coal face spalling usually occurs in the initial weighting and periodic weighting.

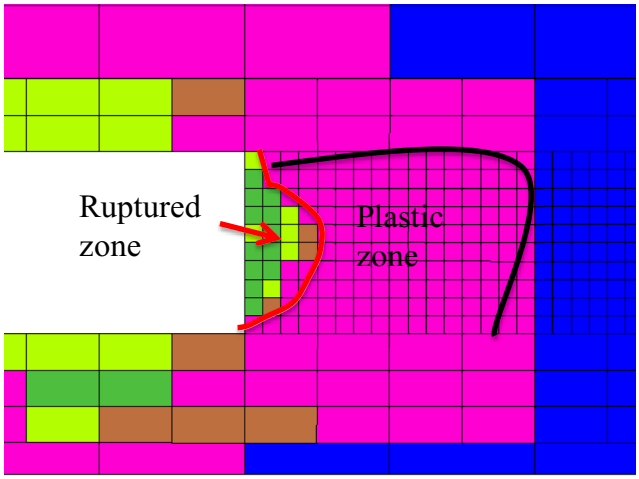

Fig. 8 Plastic damage zone of coal face

Main controlling factors of coal face spalling

Mechanical model

In terms of the structures of the overlying strata in the stope, two types were formed—"solid coal-collapse gangue" when the entire roof rock is supported by the support system, and "coal face-support-caving waste rock" when the upper roof rock adjacent to the coal seam is supported by the support system—in the advance direction after the excavation of coal mass in the working face. Therefore, the coal face and support system mainly absorb the roof pressure if the immediate and main roof are unstable. Figure 9(a) illustrates the mechanical model with a "coal face-support-roof" to investigate the stability of the coal face, and a simplified type is shown in Fig. 9(b). Assuming that the height of sliding coal M_1 reaches the maximum value M, which is the mining height of the working face, the shear force S and normal force N of the sliding surface, the shear force T on the failure face can be shown as follows.

$$S = [(Q-P+G)\cos\beta + (f-Q_0)\sin\beta] \quad (1)$$

$$N = [(Q-P+G)\sin\beta + (f-Q_0)\cos\beta] \quad (2)$$

$$T = [(Q-P+G)\sin\beta + (f-Q_0)\cos\beta]\tan\varphi + cM\sec\beta \quad (3)$$

where Q is the pressure of overlying strata; P is the support system working resistance; G is the gravity of the sliding body; f is the friction between the coal body and immediate roof; Q_0 is the force acting on the coal face caused by the support plate; β and φ are the failure angle and internal friction angle of the coal body, respectively; c is cohesive force; and M is the mining height.

Combined with Eqs. (1)–(3), the stability coefficient K of the coal face can be defined as follows.

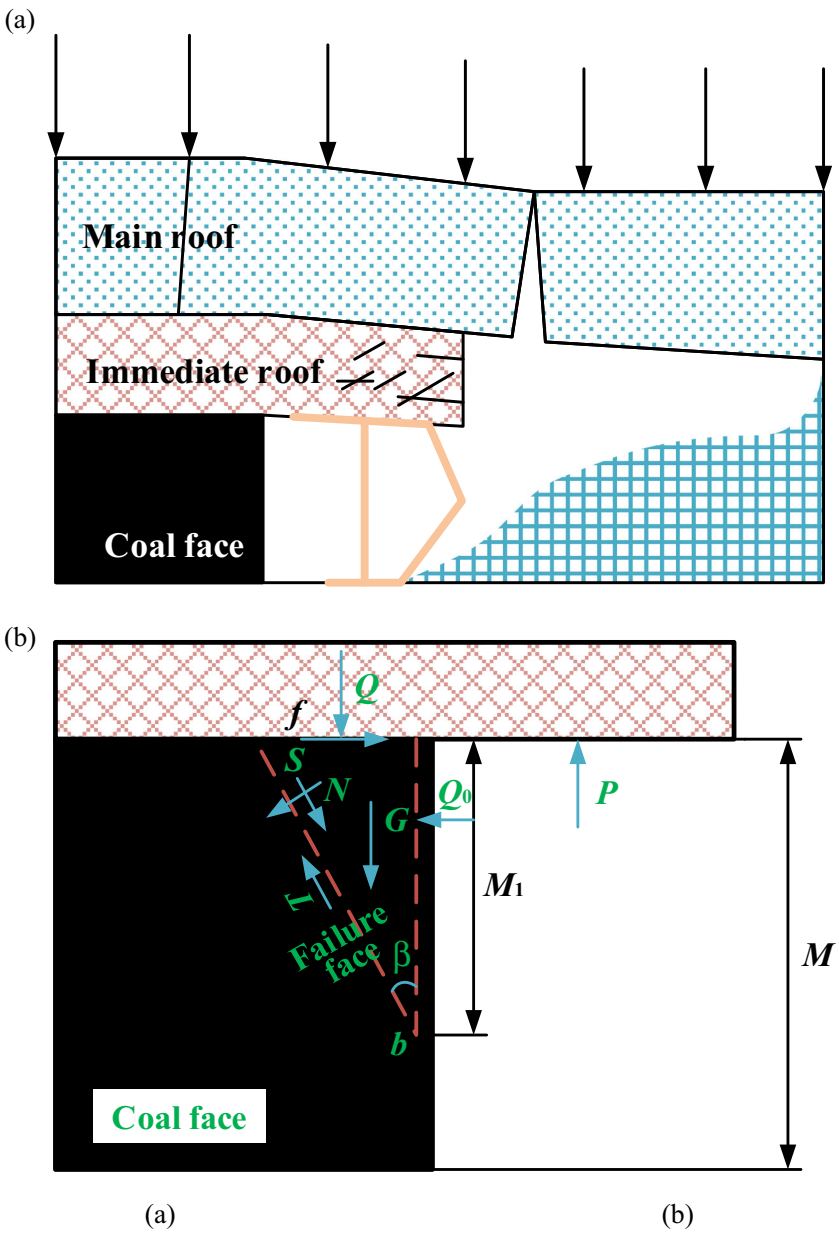

Fig. 9 Mechanical model: (a) coal face-support-roof, (b) simple model

$$K = \frac{T}{S} = \frac{[(Q-P+G)\sin\beta + (f-Q_0)\cos\beta]\tan\varphi + cM\sec\beta}{[(Q-P+G)\cos\beta + (f-Q_0)\sin\beta]} \quad (4)$$

Clearly, many factors together determine the stability coefficient according to Eq. (4). Firstly, as the value of roof pressure Q increases, the likelihood of coal face instability increases as well. The former is related to mining height and mining depth, which affect the value of horizontal stress. Therefore, it can be said that the stability of the coal face is directly dependent on the mining height and horizontal stress in the working face.

Secondly, the coal face and support system jointly bear the pressure of the overlying strata. Therefore, the pressure of the coal face bore and the friction between the coal body and immediate roof are minimal if a good support system can fully be mobilized to increase the stability of the coal face.

Thirdly, the cohesion and internal friction angle of the coal mass also play a vital role in the stability of the coal face. The weak strength of the coal mass is prone to cause coal face failure easily. Therefore, a large-cutting-height working face with a deep-buried seam is likely to cause coal face spalling due to the low strength of coal and rock mass in a deep coal mining face.

mmary, horizontal stress, mining height, support system working resistance and coal strength act on the stability of

Table 2 Joint mechanical parameters of coal and rock mass

Rock	Jkn (MPa)	Jks (MPa)	Jfri (°)	Jcoh (MPa)	Jten (MPa)
Coarse sandstone	6368	5840	25	3.12	2.08
Medium sandstone	5500	5960	22	2.38	1.56
Siltstone	4540	4800	19	1.85	0.86
Fine sandstone	3600	4380	18	1.27	0.75
Mudstone	2550	2240	17	0.86	0.22
Coal seam	2350	2320	15	0.45	0.04

the coal face together. However, it is difficult to analyze the main controlling factors using only theoretical methods. Therefore, in order to develop specific control measures for resolving coal face failure, it is necessary to perform numerical simulation to investigate the relative importance of these factors.

Analysis of the main factors affecting the stability of a coal mining face

Taking panel 1303 as engineering background, the two-dimensional Universal Distinct Element Code (UDEC^{2D}) software program was used to investigate the influence of cutting height, horizontal stress, support working resistance, and the cohesion and internal friction angle of a coal mass on the stability of the coal mining face. Figure 10 presents the basic numerical model. The mechanical parameters of the coal and rock mass are shown in Table 1 as well. Following the work of some scholars (Cai et al. 2013), in combination with the laboratory testing results, the joint physical and mechanical parameters of the coal and rock mass are shown in Table 2.

Mining depth

The mining depth was simulated in the numerical model by changing the vertical loading and lateral pressure. Specifically, a vertical loading coefficient of 20, 15, 10 and 5 MPa and a lateral pressure coefficient of 1.6, 1.2, 0.8 and 0.4 were adopted to simulate different mining depths of 800, 600, 400 and 200 m, respectively.

As shown in Figs. 11 and 15(a), which illustrate the influence of mining depth on the failure characteristics of a coal mining face, the maximum failure depth and failure zone of the coal mining face is 0.5 m and 1.2 m^2, respectively, if the mining depth is 200 m. An increase from 0.8 m to 1.1 m followed by 1.5 m, and from 2.3 m^2 to 3.6 m^2 followed by 5.6 m^2, are revealed in terms of the maximum failure depth and failure zone, respectively. Therefore, it is concluded that the failure depth and failure zone increase significantly with increased mining depth. However, the shear failure in the top part of the coal mining face occurs mainly at a shallow burial depth, while the occurrence of coal face spalling with the entire height of the coal mining face combined with tensile and shear failure can be demonstrated with a continuous increase in mining depth.

Mining height

Four different mining heights were utilized in numerical simulation, and the results with an advance distance of 50 m are shown in Fig. 12. The maximum failure depth and failure zone increase from 0.7 m to 1.0 m, 1.5 m and finally to 1.7 m, and from 1.5 m^2 to 3.4 m^2, 5.6m^2 and finally to 7.4 m^2, respectively, with the increase in mining height from 3 m to 4 m, 5 m, and finally to 6 m, as shown in Fig. 15(b). Clearly, the failure depth and failure zone area of the coal mining face increase marginally with an increase in mining height, and

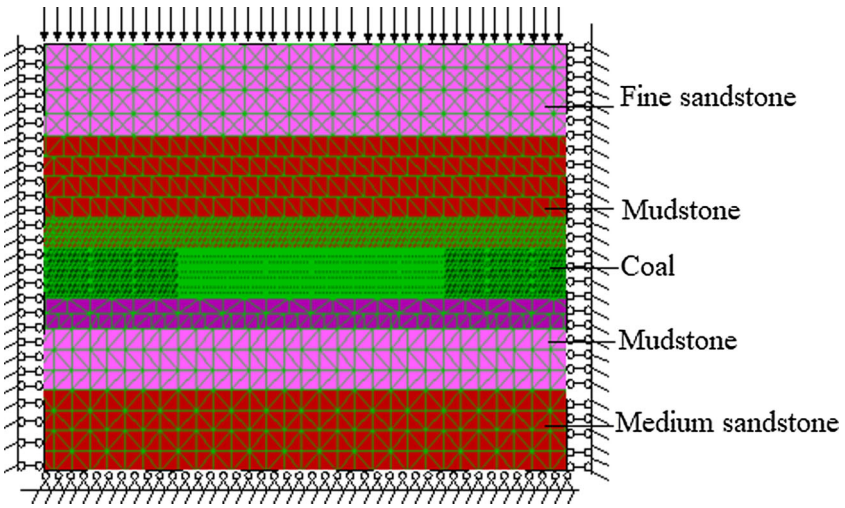

Fig. 10 Numerical simulation model

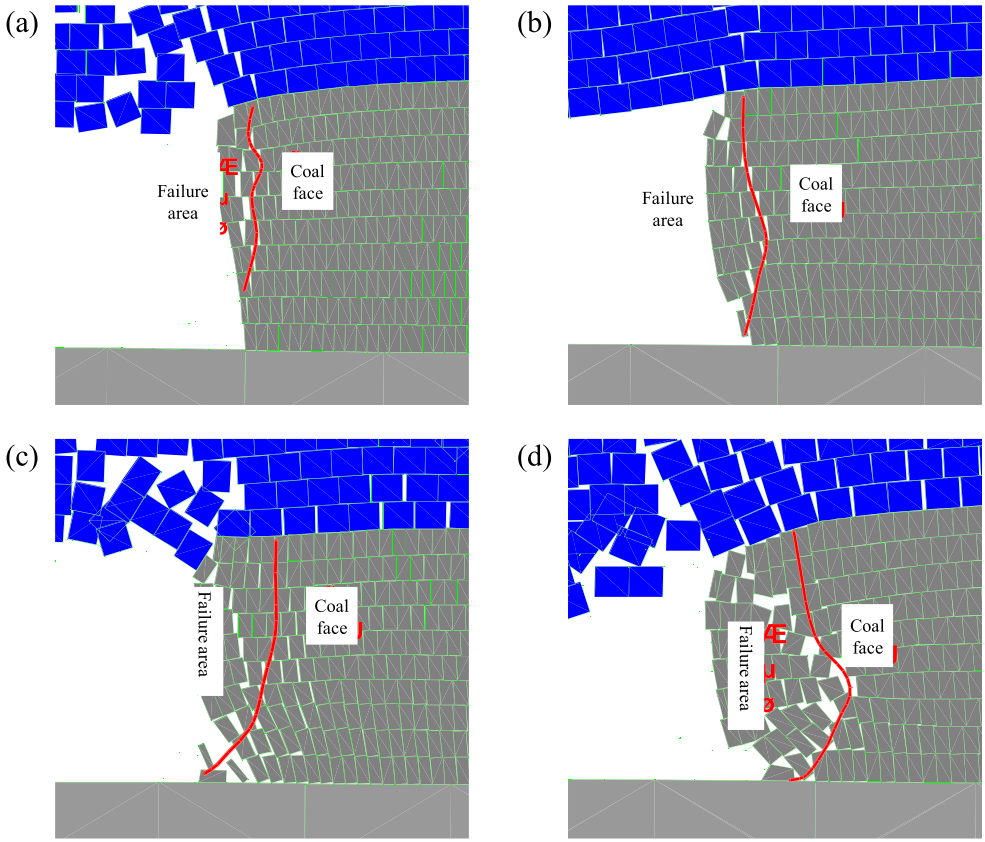

Fig. 11 Failure features of the coal mining face with mining depths of (a) 200 m, (b) 400 m, (c) 600 m, (d) 800 m

all four mining heights cause failure of the whole height of the coal face. Meanwhile, the adjustable range of mining height is also limited in a specific mining face. Therefore, the mining height plays a minor role in coal face spalling; as a result, reducing the mining height does not fundamentally change the degree of failure of the coal mining face.

Cohesion of the coal mass

Figure 13 illustrates the failure features of the coal face with different values of coal body cohesion. The sliding surface is marked by the red line, which reveals that the maximum failure depth and failure zone area decreased from 2.1 m to 1.5 m, and from 8.3 m^2 to 5.6 m^2, respectively, if the cohesion of coal mass increased from 0.5 MPa to 1 MPa. There was almost no apparent failure in the working face with the cohesion increasing to 3 MPa, as shown in Fig. 15(c). Therefore, the weak strength of a coal body in deep mining can also be regarded as the main reason for coal face spalling. The stability of the coal face can be significantly improved and controlled with an increase in coal mass cohesion.

Support strength

In terms of a support system, the support strength can also affect the stability of a coal face to some degree, as shown in Fig. 14. The maximum failure depth and failure zone are 1.5 m and 5.6 m^2, respectively, without support strength. If the support strength increases from 1.0 MPa to 1.25 MPa, and finally to 1.5 MPa, the corresponding maximum failure depth and failure zone decrease from 1.3 m to 1.1 m, and finally to 0.8 m, and from 4.5 m^2 to 2.8 m^2, and finally to 2.3 m^2, respectively, as shown in Fig. 15(d). It is concluded that the degree of failure of a coal face can be reduced with an increase in support strength, and its rate decreases. Therefore, the role of increasing support strength to improve the stability of a coal face is also fundamentally limited.

For demonstrating the main factors affecting the failure depth and failure zone area of a coal mining face in detail, the normalization method was adopted to deal with different factors in the range of 0 to 1 using Eq. (5), as shown in Fig. 16.

$$x^* = \frac{x - x_{\min}}{x_{\max} - x_{\min}} \tag{5}$$

where x^* and x are the normalization value and reality value of different main factor parameters, respectively. $x_{\min}$ and $x_{\max}$ are the minimum and maximum values of each factor parameter, respectively.

As shown in Fig. 16(a), cohesion (C) mainly contributes to the increase in the degree of failure depth (FD). The mining depth (MD) and mining height (MH) exhibit a similar trend to restrict the occurrence of coal face spalling, while the weakest

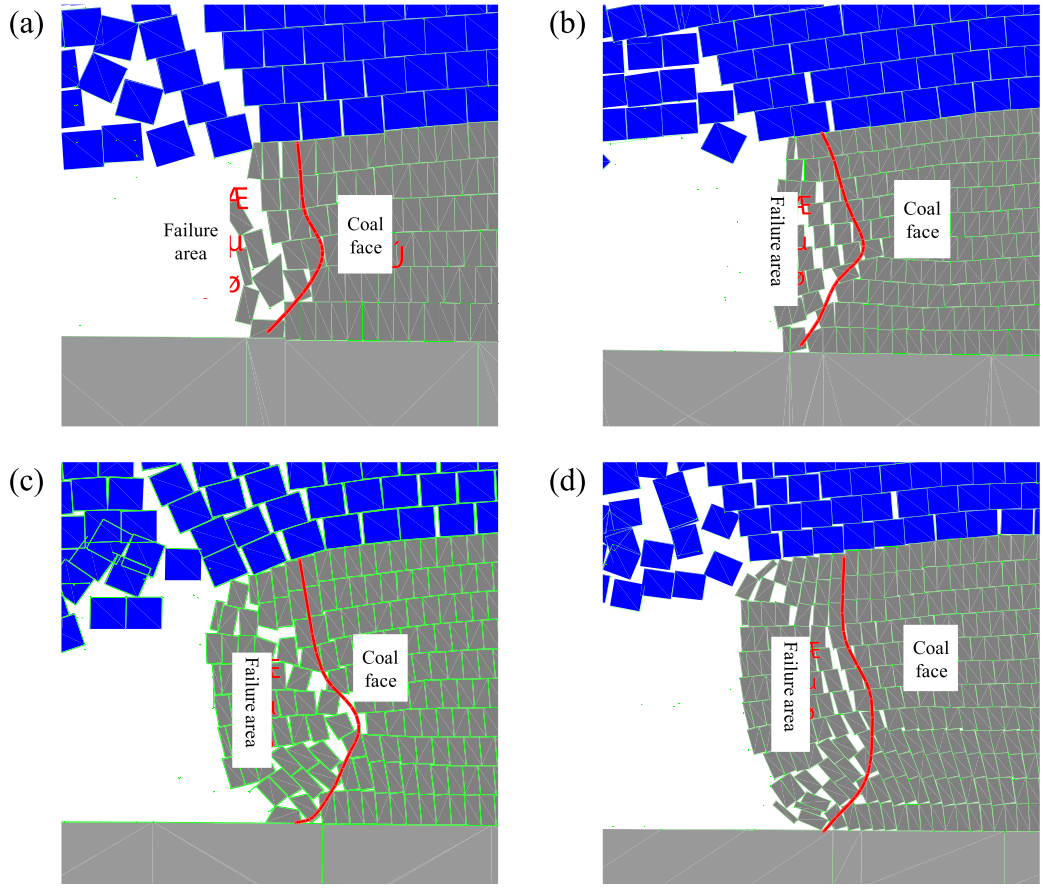

Fig. 12 Failure features of the coal mining face with mining heights of (a) 3 m, (b) 4 m, (c) 5 m, (d) 6 m

impact factor on the failure depth of a coal mining face is illustrated by the support strength (SS). However, in terms of failure area (FA), with the most predominant and weakest factors unchanged, the influence of mining height on failure area is greater than that of mining depth. Thus it can be concluded that the four main factors influencing coal face stability can be ranked as follows: cohesion (S) > mining height (MH) > mining depth (MD) > support strength (SS).

Stability control technology for a coal face

Based on the results of numerical simulation, it can be concluded that the strength of a coal body, mining height and mining depth are of great importance to the stability of a coal face, while support strength has limited influence. Therefore, targeted measures can be proposed and implemented for controlling coal face spalling in a large-cutting-height mining face with a deep-buried seam. In general, a zone with no serious failure in a coal face adopts general control measures as follows:

1) Firstly, it is necessary to determine the reasonable mining height and the length of the working face as well as advance speed. Obviously, the potential for coal face failure is positively correlated with mining height influencing the action range of abutment pressure and the length of the working face influencing roof pressure, while increasing advance speed can reduce the action time of roof pressure on the coal face to further improve the stability of the coal face. On the other hand, mining height and the length of the working face are crucial parameters to guarantee the production capacity of a coal mining face. Therefore, the selected values of mining height, the length of the working face, and advance speed need to be balanced for both safety and production capacity.
2) Secondly, improving the initial support strength can be effective in maintaining the stability of a coal face because the strength of a coal face bore decreases. Moreover, the mobilization of a support plate can change the stress state of a coal body from two dimensions to three dimensions, further increasing the strength of a coal body. Therefore, the effective control of coal face spalling and the sliding zone in a coal face can be realized by taking full advantage of support plates.
3) Thirdly, injecting water into a coal seam to improve the cohesion of a coal body increases the strength of a coal mass and also enhances the stability of the coal face

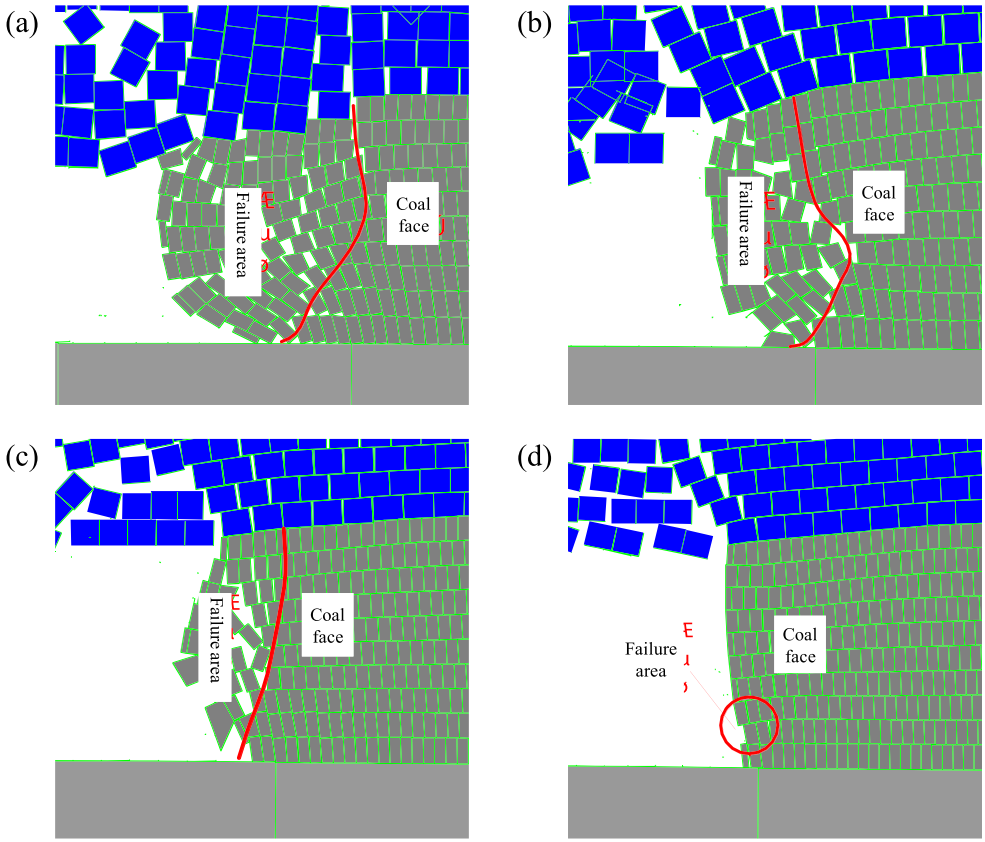

Fig. 13 Failure features of a coal mining face with cohesion values of (a) 0.5 MPa, (b) 1 MPa, (c) 1.5 MPa, (d) 3 MPa

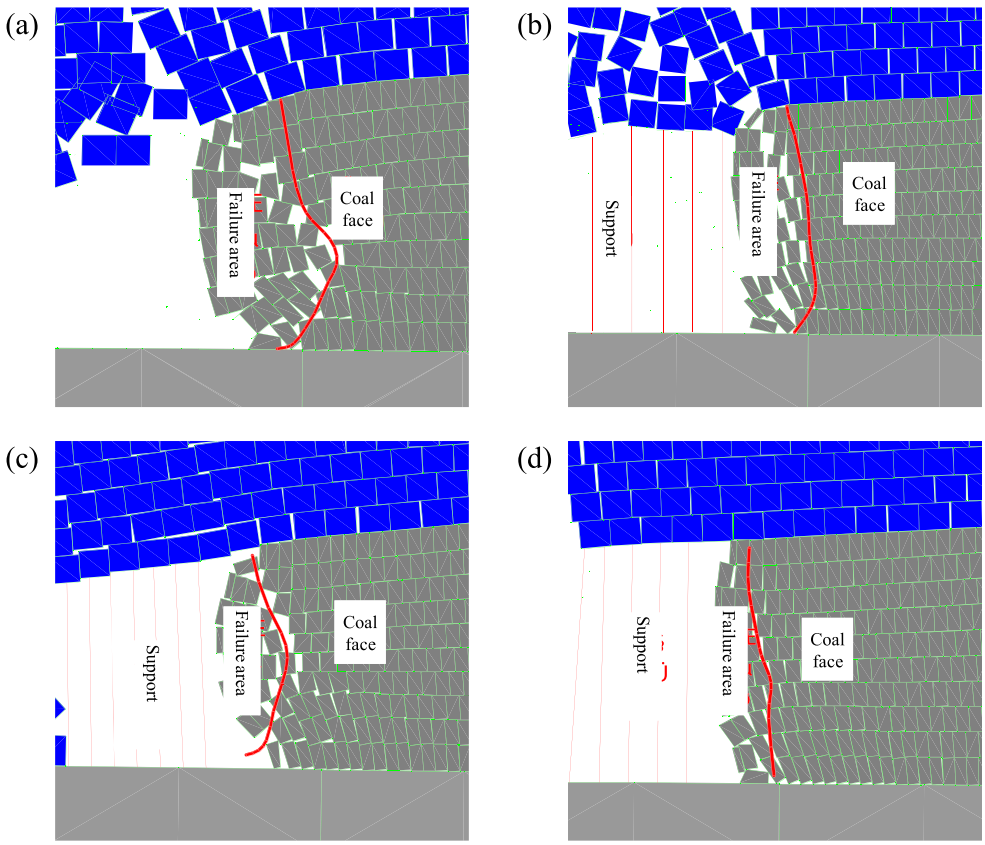

Fig. 14 Failure features of a coal mining face with support strength of (a) 0 MPa, (b) 1.0 MPa, (c) 1.25 MPa, (d) 1.5 MPa

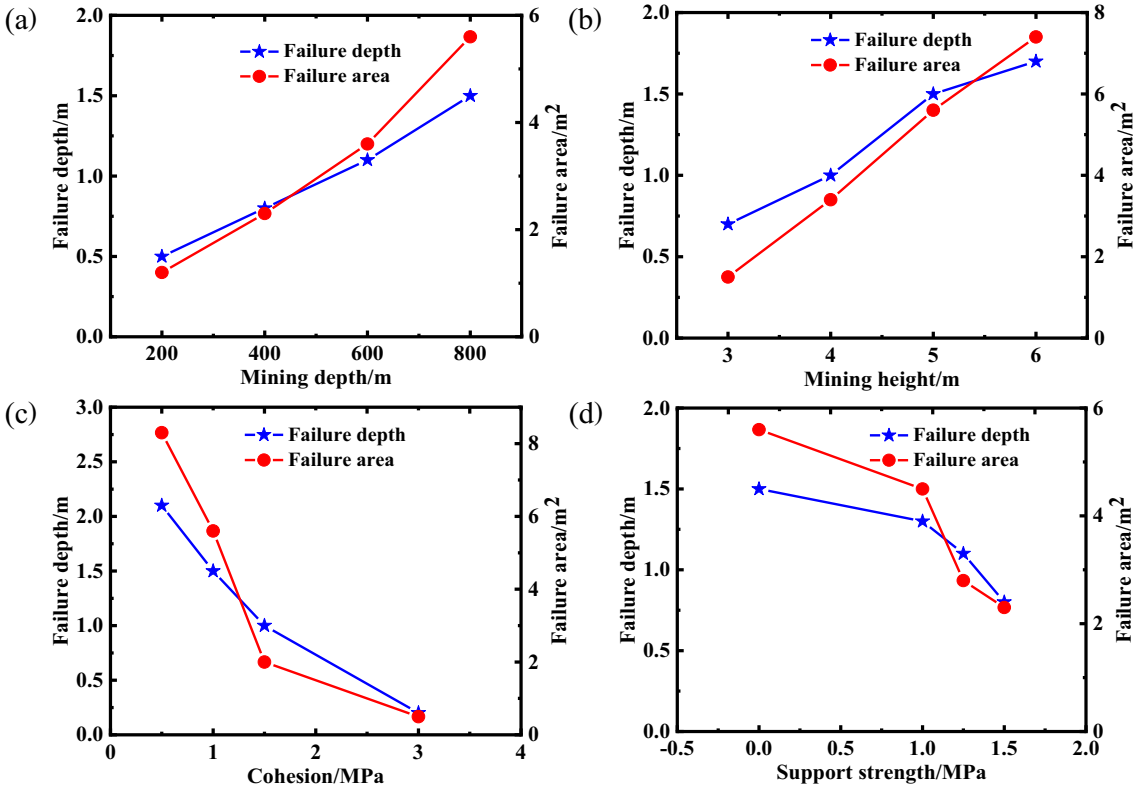

Fig. 15 Main factors affecting the failure depth and failure zone area of a coal mining face: (a) mining depth, (b) mining height, (c) cohesion, (d) support strength

because the bearing capacity of a coal face depends on the strength of the coal mass, and leads to different forms of failure, such as tensile failure or shear failure.

In terms of some specific engineering geology conditions, such as a large-cutting-height and deep-buried mining face with the failure characteristics of asymptotic, periodic and larger deformation, the general control measures

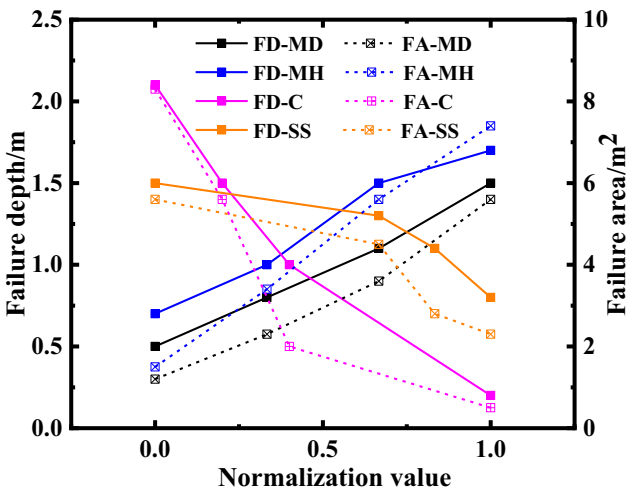

Fig. 16 Normalization of main factors affecting the stability of a coal mining face

like those mentioned above are not sufficient to maintain the stability of a coal face. Therefore, the technology using "manila + grouting" reinforcement into a coal mass is proposed to control the serious area in a coal face and roof caving, as shown in Fig. 17. The principle for proposing the "manila + grouting" reinforcement technology is that the slurry of flexible reinforcement can densely fill the coal body in plastic and fracture zones to improve the integrity of the coal face; it also restores the coal body to an approximately elastic state. Thus the principal factor of cohesion can be significantly increased by adopting this technology, and it can be effective and efficient for resisting the passive effect of plastic deformation.

1) A roof bolter with a 42-mm bit diameter is used to drill the length and angle in a vertical direction to 5 m and 10°–15°, respectively, at a position 3 m from the floor. The horizontal distance and offset between two holes are 5 m and 10°–15°, respectively.
2) The tensile strength and elongation of manila adopted with the diameter of 12 mm are 3–8 MPa and 12–15%, respectively, and the grouting pressure is in the range of 3–8 MPa. The grouting pipe is made of plastic material with a diameter of 20 mm. Figure 17(b) represents the arrangement of manila and grouting pipe in the form of a tangent circle.

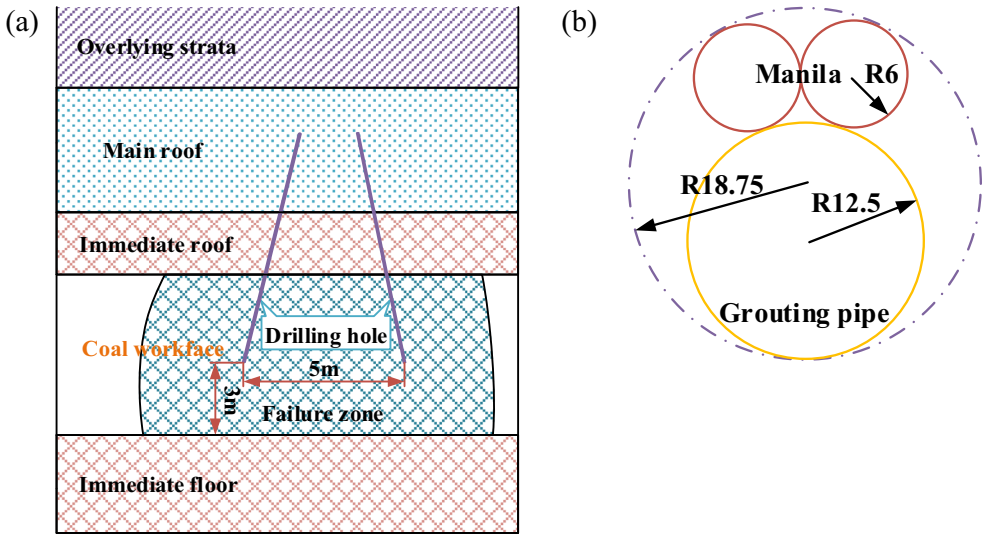

Fig. 17 The site operation of "manila + grouting" reinforcement technology: (a) drilling arrangement, (b) the connection arrangement between manila and grouting pipe

Compared with only the general measures adopted, coal face stability improved significantly by applying "manila + grouting" reinforcement into the coal body in panel 1303, with the maximum failure depth and failure zone greatly reduced. Furthermore, the potential for coal face spalling and the failure degree of a coal face are reduced by 70–80%, and grouting costs are reduced by save 30–40%.

Conclusions and future work

Based on the engineering background of panel 1303, this paper presents the failure mechanism and stability control measures of a large-cutting-height coal mining face with a deep-buried seam combined with laboratory experiments, theoretical calculation, numerical simulation and field application. The following conclusions can be drawn from the present study.

The stress environment of a coal face plays a vital role in coal face spalling because it is caused by the cyclic normal stress as well as the continuous unloading of confining pressure in the process of excavation. Especially before the period of initial weighting, the strength of a coal mass gradually decreases due to the stress state of the coal face changing from three dimensions to two dimensions, or even one dimension, causing the instability of the coal face. In terms of panel 1303, two-dimensional loading can be revealed in front of the coal face within 3 m. Moreover, the principal horizontal stress σ_{yy} is greater than the principal vertical stress σ_{zz} followed by σ_{xx} in the front of a coal face within 8 m.

The strength of a coal mass, mining height and mining depth can be regarded as the main factors influencing the stability of a coal face in a large-cutting-height working face with a deep-buried seam compared with support strength.

Compared with conventional control measures for coal face spalling with no obvious effects, the failure degree of a coal face is reduced 70–80%, and grouting costs are reduced by 30–40% with the use of the 'manila + grouting' reinforcement into the coal face. Therefore, it can be concluded that this technical innovation exerts an apparent inhibitory effect on the occurrence of coal face spalling.

However, it should also be noted that these conclusions are focused on the failure mechanism and stability control measures of a large-cutting-height coal mining face using engineering knowledge obtained from panel 1303. Therefore, possible effects may be caused by other mechanical inputs that should be analyzed in further studies.

Acknowledgements The authors wish to acknowledge financial support from the Scientific Research Foundation of Guizhou Provincial Department of Science & Technology and Guizhou University (QianKehe LH [2017]7280), Annual Academic Training and Special Innovation Program of Guizhou University in 2017 (Guizhou Kehe [2017]5788), the Fund of Key Laboratory of Safety and High-efficiency Coal Mining, Ministry of Education (JYBSYS2017101) and the China Scholarship Council. The authors would also like to thank the editors and anonymous reviewers for their valuable time and suggestions.

References

Aguado MBD, González C (2009) Influence of the stress state in a coal bump-prone deep conalbed: a case study. Int J Rock Mech Min Sci 46(2):333–345. https://doi.org/10.1016/j.ijrmms.2008.07.005

Alejano LR, Ramírez-Oyanguren P, Taboada J (1999) FDM predictive methodology for subsidence due to flat and inclined coal seam mining. Int J Rock Mech Min Sci 36(4):475–491. https://doi.org/10.1016/S0148-9062(99)00022-4

Asadi A, Shakhriar K, Goshtasbi K (2004) Profiling function for surface subsidence prediction in mining inclined coal seams. J Min Sci 40(2):142–146. https://doi.org/10.1023/B:JOMI.0000047856.91826.76

Cai MF, HE MC, Liu DY (2013) Rock mechanics and engineering. Science Press, Beijing (in Chinese)

Chang JC, Xie GX, Zhang XH (2015) Analysis of coal face spalling mechanism of fully-mechanized top-coal caving face with great mining height in the extra-thick coal seam. Rock Soil Mech 36(3): 803–808. https://doi.org/10.16285/j.rsm.2015.03.026

Christopher M (2016) Coal bursts in the deep longwall mines of the United States. Int J Coal Sci Technol 3(1):1–9. https://doi.org/10.1007/s40789-016-0102-9

Fan X, Kulatilake PHSW, Chen X (2015) Mechanical behavior of rock-like jointed blocks with multi-non-persistent joint under uniaxial loading: a particle mechanics approach. Eng Geol 190:17–32. https://doi.org/10.1016/j.enggeo.2015.02.008

Gao FQ, Stead D (2014) The application of a modified Voronoi logic to brittle fracture modelling at the laboratory and field scale. Int J Rock Mech Min Sci 68:1–14. https://doi.org/10.1016/j.ijrmms.2014.02.003

Gao F, Stead D, Kang H (2014a) Simulation of roof shear failure in coal mine roadways using an innovative UDEC trigon approach. Comput Geotech 61(3):33–41. https://doi.org/10.1016/j.compgeo.2014.04.009

Gao F, Stead D, Kang H, Wu Y (2014b) Discrete element modelling of deformation and damage of a roadway driven along an unstable goaf–a case study. Int J Coal Geol 127(7):100–110. https://doi.org/10.1016/j.coal.2014.02.010

He MC, Sousa LR, Miranda T, Zhu GL (2015) Rockburst laboratory tests database-application of data mining technique. Eng Geol 185:116–130. https://doi.org/10.1016/j.enggeo.2014.12.008

Huang BX, Li HT, Liu CY, Xing SJ, Xue WC (2011) Rational cutting height for large cutting height fully mechanized top-coal caving. Min Sci Technol 21:457–462. https://doi.org/10.1016/j.mstc.2011.05.020

Iannacchione AT, Tadolini SC (2016) Occurrence, predication, and control of coal burst events in the U.S. Int J Min Sci Technol 26:39–46. https://doi.org/10.1016/j.ijmst.2015.11.008

Kazerani T (2013) Effect of micromechanical parameters of microstructure on compressive and tensile failure process of rock. Int J Rock Mech Min Sci 64:44–55. https://doi.org/10.1016/j.ijrmms.2013.08.016

Kong DZ, Yang SL, Gao L, Ma ZQ (2017) Determination of support capacity based on coal face stability control. J China Coal Soc 42(3):590–596. https://doi.org/10.13225/j.cnki.jccs.2016.1296

Li XP, Kang TH, Yang YK, Li H, Li CY, Wu LL, Du MZ (2015) Analysis of coal face slip risk and caving depth based on bishop method. J China Coal Soc 40(7):1498–1504. https://doi.org/10.13225/j.cnki.jccs.2014.0912

Li XH, Ju MH, Yao QL, Zhou J, Chong ZH (2016) Numerical investigation of the effect of the location of critical rock block fracture on crack evolution in a gob-side filling wall. Rock Mech Rock Eng 49(3):1041–1058. https://doi.org/10.1007/s00603-015-0783-1

Lisjak A, Grasselli G (2014) A review of discrete modeling techniques for fracturing processes in discontinuous rock masses. J Rock Mech Geotech Eng 6:301–314. https://doi.org/10.1016/j.jrmge.2013.12.007

Mazaira A, Konicek P (2015) Intense rockburst impacts in deep underground construction and their prevention. Can Geotech J 52:1426–1439. https://doi.org/10.1139/cgj-2014-0359

Pang YH, Wang GF (2017) Hydraulic support protecting board analysis based on coal face spalling "tensile cracking-sliding" mechanical model. J China Coal Soc 42(8):1941–1950. https://doi.org/10.13225/j.cnki.jccs.2016.1696

Peng SS, Chiang HS (1984) Longwall mining. John Wiley and Sons, Inc., New York

Suorineni FT, Mgumbwa JJ, Kaiser PK, Thibodeau D (2014) Mining of orebodies under shear loading part 2–failure modes and mechanisms. Min Technol 123(4):240–249. https://doi.org/10.1179/1743286314Y.0000000072

Wang JC, Wang L, Guo Y (2014) Determining the support capacity based on roof and coal face control. J China Coal Soc 39(8):1619–1624. https://doi.org/10.13225/j.cnki.jccs.2014.9027

Wang JC, Wang ZH, Kong DZ (2015) Failure and prevention mechanism of coal face in hard coal. J China Coal Soc 40(10):2243–2250. https://doi.org/10.13225/j.cnki.jccs.2015.6013

Wang JC, Yang SL, Kong DZ (2016) Failure mechanism and control technology of Longwall coal face in large-cutting-height mining method. Int J Min Sci Technol 26(1):111–118. https://doi.org/10.1016/j.ijmst.2015.11.018

Wang G, Wu MM, Wang R, Xu H, Song X (2017) Height of the mining-induced fractured zone above a coal face. Eng Geol 216:140–152. https://doi.org/10.1016/j.enggeo.2016.11.024

Xuan DY, Xu JL, Wang BL, Teng H (2016) Investigation of fill distribution in post-injected longwall overburden with implications for grout take estimation. Eng Geol 206:71–82. https://doi.org/10.1016/j.enggeo.2016.04.007

Yang SL, Kong DZ (2015) Flexible reinforcement mechanism and its application in the control of spalling at large mining height coal face. J China Coal Soc 40(6):1361–1367. https://doi.org/10.13225/j.cnki.jccs.2015.0271

Yang SL, Kong DZ, Yang JH, Meng H (2015) Coal face stability and grouting reinforcement technique in fully mechanized caving face during topple mining. J Min Saf Eng 32(5):827–833,839. https://doi.org/10.13545/j.cnki.jmse.2015.05.020

Yao QL, Li XH, Sun BY, Ju MH, Chen T, Zhou J, Liang S, Qu QD (2017) Numerical investigation of the effects of coal seam dip angle on coal face stability. Int J Rock Mech Min Sci 100:298–309. https://doi.org/10.1016/j.ijrmms.2017.10.002

Zhang L, Einstein HH (2004) Using RQD to estimate the deformation modulus of rock masses. Int J Rock Mech Min Sci 41(2):337–341. https://doi.org/10.1016/S1365-1609(03)00100-X

Zhao TB, Guo WY, Tan YL, Lu CP, Wang CW (2017) Case histories of rock bursts under complicated geological conditions. Bull Eng Geol Environ 2:1–17. https://doi.org/10.1007/s10064-017-1014-7

Zhou H, Meng FZ, Zhang CQ, Hu DW, Yang FJ, Lu JJ (2015) Analysis of rockburst mechanisms induced by structural planes in deep tunnels. Bull Eng Geol Environ 74(4):1–17. https://doi.org/10.1007/s10064-014-0696-3